Available online at www.sciencedirect.com
ScienceDirect
International Journal of Heat and Mass Transfer 51 (2008) 941–947
International Journal of HEAT and MASS TRANSFER
www.elsevier.com/locate/ijhmt

Technical Note

An experimental study of heat transfer in a two-dimensional T-junction operating at a low momentum flux ratio

A. de Tilly, J.M.M. Sousa *

Mechanical Engineering Department, Instituto Superior Técnico, Technical University of Lisbon, Av. Rovisco Pais, 1049-001 Lisboa, Portugal

Received 12 August 2007; received in revised form 5 October 2007

Abstract

A non-isothermal, two-dimensional T-junction operating at a low value of momentum flux ratio has been experimentally investigated. Mean and fluctuating measurements of temperature, coupled with a spectral analysis, have been used to characterise the dynamics of the flow for different flow conditions. A higher cooling effectiveness was found for the higher value of the Reynolds number due to an earlier development of large-scale structures. Heat transfer coefficients obtained employing the cross-flow temperature as a reference displayed an unusual behaviour. A better strategy was also proposed, taking into consideration the possible choices for the reference temperature.

Keywords: T-junction; Confluence flow; Low momentum flux ratio; Cooling effectiveness; Heat transfer coefficient; Reference temperature

1. Introduction

Confluence flows are very prone to the development of different kinds of instabilities (see e.g. [1–4]). This increases the difficulties to carry out accurate predictions of mean heat transfer in T-junctions [5]. Moreover, the fluctuating behaviour of velocity and temperature fields is often disregarded in related investigations. It is expected that supplementary investigations may improve our understanding of the dynamical phenomena involved and ultimately contribute to a better design of such flow elements.

In the work of Fukuda et al. [6], a low-momentum cold jet was discharged into a very hot cross-stream. Flow junctions employed in this context were originally designed according to traditional heat transfer coefficient calculations but the heat transfer analysis was neither appropriate nor able to anticipate thermal stripping. Coefficients for mean and fluctuating heat transfer have been obtained by Beck et al. [7] and Ogura [8], employing inverse and power spectral methods, respectively. However, these were calculated using a reference temperature which did not allow to fit the classical correlations for wall boundary layers, as noted by Noguchi et al. [9]. This is a consequence of the fact that several temperature entries exist in the flow, thus complicating the choice of a reference temperature.

It was shown by de Tilly [3] that the fluid structures strongly affect the heat transfer to the wall in these flows. These structures are usually associated with significant velocity and temperature fluctuations. On the other hand, heat transfer evolutions are traditionally correlated with mean temperatures [10]. However, Maillet [11] has pointed out that the theoretical means proposed in the literature are not adequate to model and efficiently predict heat transfer phenomena when two streams of different temperatures interact with a wall. For example, in the case of the cross-stream discharge of jets characterised by a high momentum flux ratio and different geometrical shapes, Jones [12] used several reference temperatures to model the mean heat transfer to the bounding surface.

The main objective of this experimental study is to seek physical coherence between the heat transfer to the wall and the flow behaviour in a non-isothermal, two-dimen-

* Corresponding author. Tel.: +351 21 841 7320; fax: +351 21 849 5241.
E-mail address: msousa@ist.utl.pt (J.M.M. Sousa).

0017-9310/$ - see front matter © 2007 Elsevier Ltd. All rights reserved.
doi:10.1016/j.ijheatmasstransfer.2007.10.012

Nomenclature

d	thickness of the secondary flow duct
f	frequency
h	heat transfer coefficient
H	height of the primary flow channel
J	momentum flux ratio, $J = \frac{\rho_j}{\rho_c}\left(\frac{U_j}{U_c}\right)^2$
L	length of the primary flow channel
PSD	power spectral density
r	linear correlation coefficient
Re_c	Reynolds number of the primary flow, $\frac{U_c H}{\nu}$
RMS	root mean square
s	stabilized height where the peak temperature fluctuations occur
St_d	Strouhal number based on thickness d, $\frac{fd}{U_j}$
St_s	Strouhal number based on height s, $\frac{fs}{U_j}$
T	temperature
U	mean flow velocity
w	width of the primary flow channel
x,y,z	spatial coordinate

Greek symbols

ϕ	heat flux
ν	kinematic viscosity
θ_w	cooling effectiveness

Subscripts

a	ambient
c	cross-flow, primary flow
iso	isothermal
j	jet, secondary flow
w	wall

sional T-junction, operating at a low value of momentum flux ratio. A contribution to improve our understanding of the origins of thermal stripping in non-isothermal T-junctions is also aimed at with the present investigations. Mean and fluctuating measurements of temperature, as well as power spectra, are used to characterise the dynamics of the flow for three different values of the Reynolds number. Subsequently, these results are integrated into the estimation and interpretation of mean heat transfer coefficient evolutions, considering the possible choices of reference temperature.

2. Experimental setup

2.1. Description of the test section and conditions

A schematic representation of the confluence zone is shown in Fig. 1. Electronically-controlled air heaters located upstream (not shown) allowed to maintain inlet temperatures constant during the experiments. By changing the value of U_c, the Reynolds number Re_c characterising the primary channel flow could be varied among the values of 6500, 13,000 and 19,500. The secondary flow velocity U_j was adjusted to obtain a low value of the jet momentum flux ratio, which was defined as $J = \rho_j U_j^2/\rho_c U_c^2$. A distinctive feature of the present investigation is the fact that a low value of the momentum flux ratio has been considered, namely $J = 0.01$.

The test section has an effective length $L = 300$ mm along the x-direction. The height and width of this channel are $H = 50$ mm and $w = 250$ mm, respectively. The duct from which the secondary flow emerges into the cross-stream spans the whole width of the main channel as a slot of constant thickness, $d = 15$ mm. Based on the large value of the ratio w/d, three-dimensional effects have been neglected. Consequently, only measurements at a plane located at the channel mid-span ($z = 0$) have been performed in this study and the whole analysis carried out in this paper has been made under the assumption of two-dimensional flow.

The flow upstream the confluence zone was approximately uniform due to a 1:20 contraction, and the free-stream turbulence level was kept at a nearly constant value of 2%. However, aiming to examine also the influence of the turbulence intensity on the mixing phenomena, a grid turbulator has been installed at the exit of the primary channel contraction in part of these experiments. In such cases, the turbulence level has been increased to roughly 10% in the vicinity of the jet slot.

Temperature measurements were conducted both for the case of streams with the same temperature ("isothermal") and non-isothermal cases, with especial emphasis on the latter. The "isothermal" case was characterised by the following temperature values: $T_c = T_j = 110$ °C and $T_a = 30$ °C. The temperature difference between the flow and the ambient air was high enough so that a non-negligible amount of heat was transferred to the bottom wall of the channel. Non-isothermal cases were investigated for $T_c = 110$ °C and $T_j = T_a = 30$ °C. The studied wall sketched in Fig. 1 was constructed with a smooth, opaque, 1-cm thick Teflon® plate with the aim of minimising heat conduction in the wall along the longitudinal direction. The remaining walls in the primary channel were metallic (steel) and silver-coated to minimize heat losses by radiation from the bottom wall.

2.2. Instrumentation

Temperature measurements were made near the bottom wall of the channel depicted in Fig. 1. Aiming to characterise the evolution of time-averaged and fluctuating temperatures at different stations downstream the jet exit, a thin

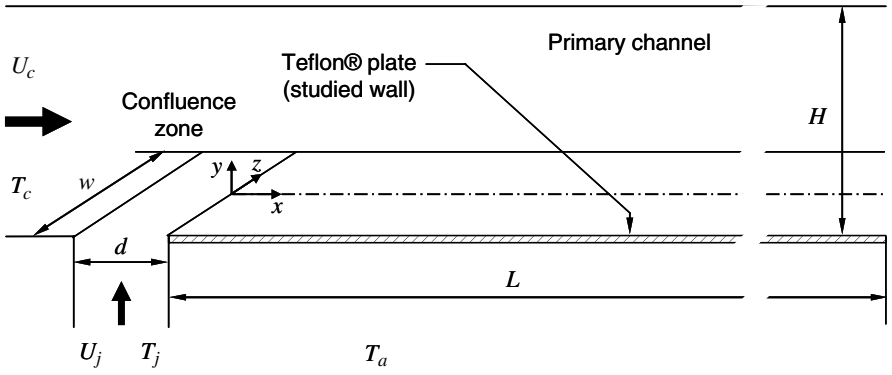

Fig. 1. Schematic representation of the confluence zone.

Chromel–Alumel thermocouple with a wire diameter of 12 μm was used. For the investigated conditions, the thermocouple has shown to be sensitive enough to describe the temperature fluctuations in the near-wall flow, and data reproducibility, which is a good indicator of the accuracy of the measurements, was, on average, within 5%. An acquisition rate of 100 Hz was employed, which was sufficient to take into account the flow dynamics in the present study as will be discussed in the next section.

A micrometrical screw was attached to the thermocouple probe, thus allowing to traverse a plane normal to the wall with steps of 0.1 mm. Thermal equilibrium has been assessed by the use of a series of thermocouples installed on the outer surface of the studied wall. Typically, a period of two hours was allowed for the stabilisation of the thermal field in order to avoid possible transients during the measurements. The temperature measurements have also been followed by a brief flow visualisation study. These results have been produced using a laser light sheet as illumination and smoke particles as tracers.

3. Temperature measurements

3.1. Time-averaged temperatures

Time-averaged temperature measurements in the wall region were obtained for the non-isothermal cases at seven x-stations downstream the jet exit, for the three values of the Reynolds number. Measurements for the intermediate value of Re_c were also conducted using the grid turbulator. Similarly to film-cooling studies, the cooling effectiveness by the jet has been defined as follows:

$$\theta_w = \frac{T_c - T_w}{T_c - T_j} \quad (1)$$

Fig. 2 shows that the values of θ_w decrease monotonically as the distance to the jet exit increases, irrespectively of the flow conditions. Analogous results have been found, e.g., by Yuen and Martinez-Botas [13], yielding to comparable values of centreline effectiveness for the lowest value of the investigated blowing ratios. In the present study, all

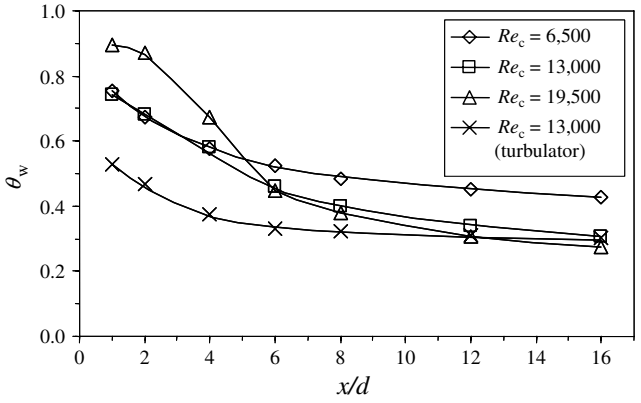

Fig. 2. Streamwise evolution of cooling effectiveness.

the cases achieve approximately the same value at $x/d = 16$, with the exception of that characterised by the lower Reynolds number. On the other hand, at the initial stations ($x/d \leqslant 4$), the case studied for $Re_c = 19{,}500$ displays a higher cooling effectiveness, whereas the grid turbulator case exhibits always the lower values in the set. Although the latter observation should not constitute a

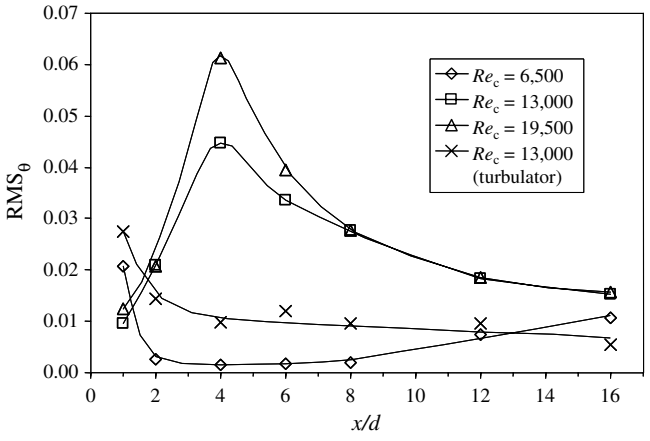

Fig. 3. Streamwise evolution of fluctuating RMS temperatures very close to the wall.

surprise due to the significant turbulent mixing occurring in the channel when the turbulator was installed, an explanation for the other situations must be sought in the unsteady features of the flow.

3.2. Temperature fluctuations

Fig. 3 shows the evolution of fluctuating RMS temperatures very close to the wall (at $y/H = 0.004$) along the various x-stations. These values have been normalised by the temperature difference between the hot and cold streams, similarly to Eq. (1). At $x/d = 1$, the larger fluctuations occur for the case with the turbulator in use ($Re_c = 13{,}000$), as might be expected. Their amplitude is seen decaying continuously along the streamwise direction. By contrast, the cases without turbulator for $Re_c = 13{,}000$ and 19,500, display the minimum value of the RMS at this initial station. However, the corresponding amplitudes increase significantly up to $x/d = 4$, where the maximum values of the set are achieved (about 40% higher for the larger value of Re_c than for the intermediate one). Both cases exhibit a similar decay in the amplitude of the temperature fluctuations further downstream.

A markedly distinct behaviour was observed in Fig. 3 for $Re_c = 6500$ (also without turbulator). The maximum RMS value is obtained at $x/d = 1$ followed by a steady decay, similarly to the findings of this study when the turbulator was in use. However, the temperature fluctuating levels are always smaller than for the latter case, except for large distances of the jet exit ($x/d \geqslant 12$) where a moderate increase of the RMS is found. Altogether, these characteristics seem to indicate that, at the lower value of the Reynolds number, a different regime of operation of the T-junction must be considered.

These results provide an explanation for the observations previously made in Fig. 2. As the value of J was always kept constant, larger values of Re_c also correspond to higher convection velocities of jet. Hence, it would be natural to expect higher values of cooling effectiveness at the initial x-stations for such cases. This was indeed noticed for $Re_c = 19{,}500$, and the nearly 50% reduction observed from $x/d = 2$ to 6 can be associated to the large temperature fluctuations occurring in this area (see Fig. 3). However, the two other cases without turbulator displayed similar values of cooling effectiveness among them despite their significantly different Reynolds numbers. The initially much larger temperature fluctuations encountered for $Re_c = 6500$ may explain these results. Consistently, a considerably higher reduction in effectiveness is observed for $Re_c = 13{,}000$ when $x/d \geqslant 4$, also corresponding to the region where the temperature fluctuations exhibited a significant increase for this case and were reduced for the lower value of Re_c (see Fig. 3). Again, the weak fluctuations measured for $Re_c = 6500$ at $x/d \geqslant 2$ may be associated to the systematically higher values of cooling effectiveness obtained for this case at the farther downstream locations ($x/d \geqslant 6$).

3.3. Flow dynamics

The spectral contents of temperature time series obtained for the various flow conditions have been analysed in an attempt to determine the origin of the distinct features described in the previous subsection. Aiming to correlate this data with the observations already made for the temperature fluctuations, time series were taken at the same (very small) distance of the wall (i.e., $y/H = 0.004$).

Fig. 4a shows power spectra obtained for $Re_c = 6500$ at three different x-stations, namely $x/d = 1$, 4 and 12. It can be observed that a well-defined, dominant frequency component is found immediately at $x/d = 1$. However, such characteristic is no longer found at the other locations further downstream. This illustrates the organised nature of the temperature fluctuations occurring at a short distance downstream of the injection (see Fig. 3). As might be anticipated, the power spectra obtained at the same spatial positions for $Re_c = 13{,}000$ and 19,500 display completely different characteristics. In Fig. 4b only the power spectra for the intermediate value of this parameter are shown, but the results for $Re_c = 19{,}500$ were qualitatively similar. In agreement with previous findings, it can be seen that the energy associated to the temperature fluctuations increases dramatically from $x/d = 1$ to 4 and then decreases further downstream. Yet, for these cases, the energy is

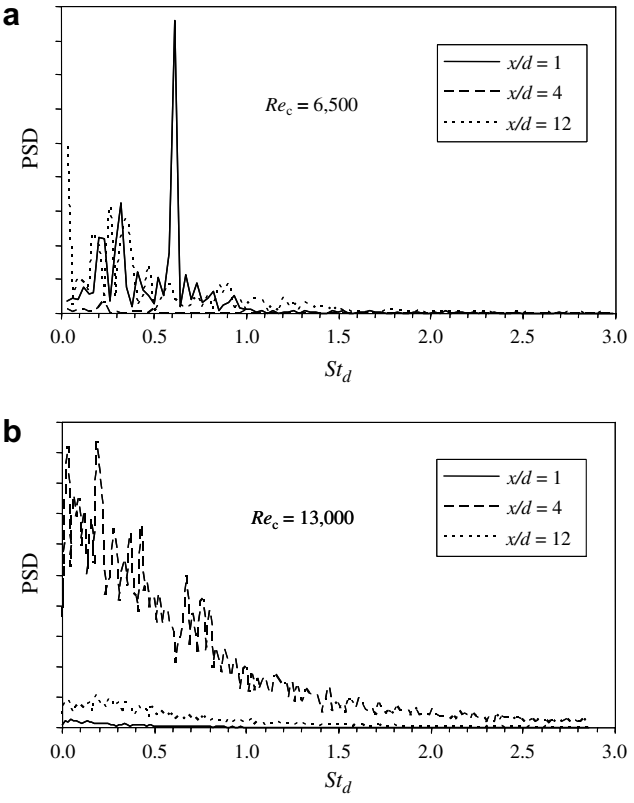

Fig. 4. Power spectra measured at $x/d = 1$, 4 and 12. (a) $Re_c = 6500$, (b) $Re_c = 13{,}000$. Power Spectral Density (PSD) scale is arbitrary.

much more distributed across the spectra, which in fact displays a clear broadband character.

The flow dynamics for the two larger values of Re_c seems to be dominated by large-scale structures resulting from the instability of the free shear layer, which is known to be broadband [14]. This process is most likely initiated in the interface between the slower wall-layer and the faster cross-flow, shortly after the jet exit. As the large-scale structures grow in size from this location, these eventually reach the wall, efficiently transporting hot fluid to this area and giving rise to high-amplitude temperature fluctuations. Visual evidence of this mechanism was obtained via flow visualisation. Fig. 5 depicts a snapshot of flow, obtained for $Re_c = 13{,}000$, where the presence of the large-scale structures is clearly noticeable and their interaction with the wall can in fact be seen occurring at about $x/d = 4$.

In contrast with the foregoing regime, large-scale structures did not seem to develop in the free shear layer for $Re_c = 6500$, at least upstream of the station $x/d = 8$. The interface between the wall-layer and the cross-flow appeared mostly quiescent for a long distance to the jet exit. Hence, as the temperature fluctuations characterising this regime were found as early as at $x/d = 1$, these must be the result of a different type of flow instability. It is hypothesised that the flow separation that must occur for a two-dimensional configuration immediately downstream of the jet duct produces a recirculation bubble, which may get unstable and be subjected to shedding. Due to lack of contrast of the flow visualisation images in the near-wall region (and probably the very small thickness of the bubble also), the phenomenon could not be unmistakably documented. However, following the ideas of Sigurdson [15] about the similarities of this mechanism with Kármán shedding, a Strouhal number St_s characterising the fluctuations was constructed. As characteristic velocity and length scales, the jet velocity U_j and the stabilized height $s \approx 0.04H$ where the peak temperature fluctuations occur were chosen, respectively. The resulting value, $St_s \approx 0.08$, was found to be in good agreement with the data reported in the literature [15], which at least partially supports the present hypothesis.

4. Mean heat transfer

After the identification and dynamical characterisation of different flow regimes in the non-isothermal confluence flow for a low value of J, the mean heat transfer to the bottom wall of the channel is investigated. The mean wall heat fluxes are evaluated under the assumption that the heat transfer between the fluid and the wall occurs by conduction only, in a very thin sub-layer adjacent to the wall. The validity of this approach has been assessed by quantifying the linearity of the mean temperature profile in the aforementioned region, typically considering five pointwise measurements. Large values of the (linear) correlation coefficient, $r^2 > 0.95$, were always obtained for $x/d \geqslant 2$, except for the case characterised by $Re_c = 19{,}500$. As a consequence, results for this condition or at the location $x/d = 1$ are not presented in the remainder of this study. However, this is not seen as a major shortcoming of the present work because it was demonstrated in the previous section that the cases for the minimum and intermediate values of Re_c already represent two distinct regimes.

Streamwise evolutions of the heat transfer coefficients for the "isothermal" experiments (h_{iso}, dashed line) and the non-isothermal study (h, solid thick line) using the same reference temperature, T_c, have initially been obtained. The results for $Re_c = 6500$ and 13,000 (without and with turbulator) are shown in Fig. 6a–c, respectively. The data for h_{iso} exhibits the classical decaying behaviour of traditional correlations and fair agreement is obtained with the results of Goldstein and Yoshida [16] for large values of x/d. By contrast, the non-isothermal heat transfer coefficient generally increases with the distance to the jet exit, although it seems to converge with h_{iso}, again for large values of x/d.

The three reported cases show different stages of development but these are consistent with the previous analysis of the flow dynamics (see Section 3.3). It can be concluded that the mixing promoted by the large-scale structures in the flow for $Re_c = 13{,}000$ is very efficient. However, the use of the grid turbulator for the same value of Re_c inhibits the formation of those organised structures and mixing is carried out by small-scale turbulence only. On the other hand, the late manifestation of the large-scale structures in the regime characterised by $Re_c = 6500$, and its corresponding low level of fluctuations at the majority of the streamwise locations (see Fig. 3), might explain both the slow development and the lower values of h obtained for this regime.

In order to circumvent the difficulty of selecting the appropriate reference temperature, the ideas of Jones [12] have been followed in order to take into consideration the characteristic temperatures of both the cross-flow and the jet, i.e. T_c and T_j, respectively. This leads to a linear combination of the contribution of each stream to the wall flux by heat transfer coefficients h_c and h_j, as follows

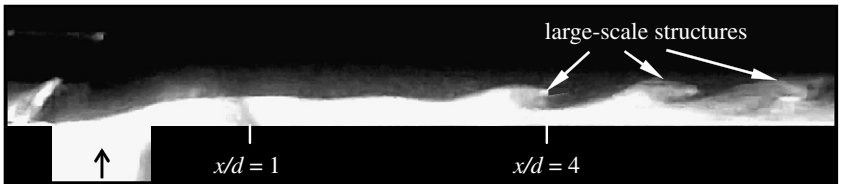

Fig. 5. Flow visualisation for $Re_c = 13{,}000$ (without grid turbulator).

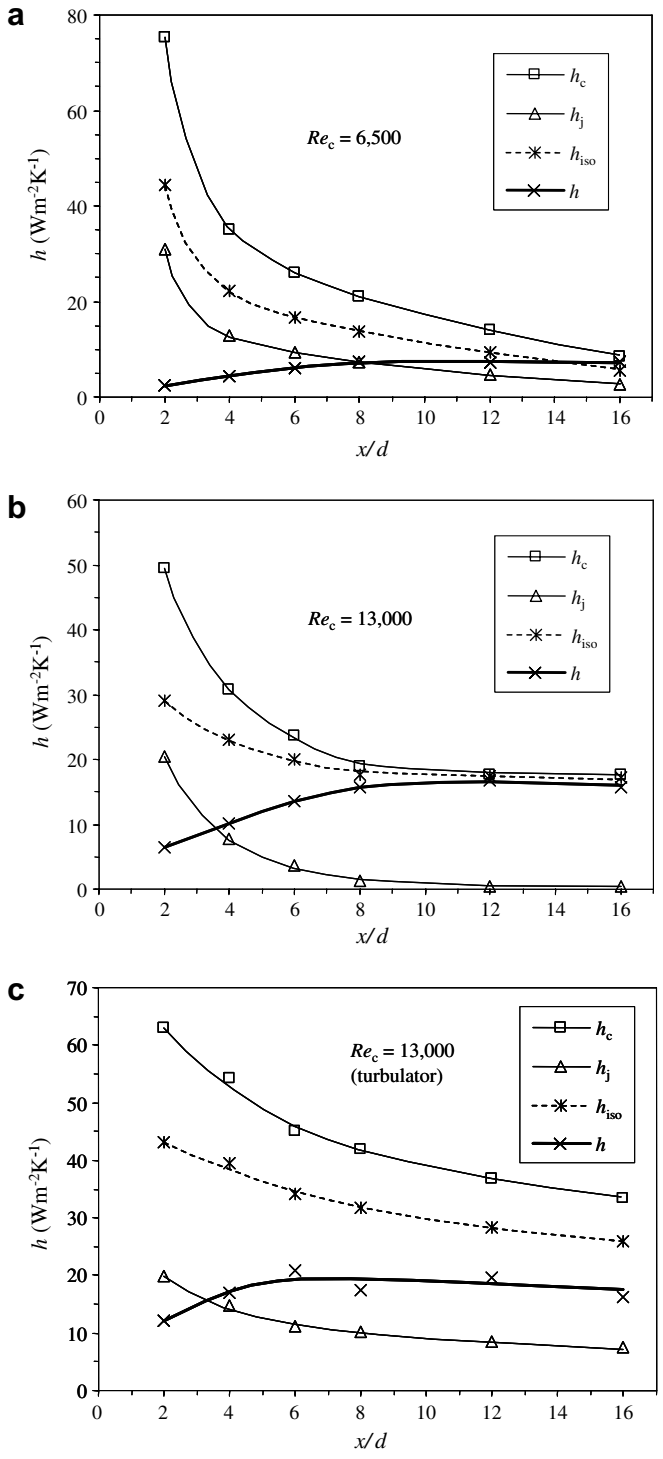

Fig. 6. Streamwise evolution of the various heat transfer coefficients. (a) $Re_c = 6500$, (b) $Re_c = 13{,}000$, (c) $Re_c = 13{,}000$ (with grid turbulator).

$$\overline{\phi_w} = h_c\overline{(T_c - T_w)} - h_j\overline{(T_j - T_w)} = (h_c - h_j)\overline{(T_c - T_w)} + h_j\overline{(T_c - T_j)} \quad (2)$$

where the overbars denote time-averaged values. Another equivalent formulation may be used to represent the heat transfer between the cross-flow and the jet by a coefficient h_1, and the heat transfer between the cross-flow and the wall by another coefficient h_2, i.e.

$$\overline{\phi_w} = h_1\overline{(T_c - T_j)} + h_2\overline{(T_c - T_w)} \quad (3)$$

The coefficient h_2 may be determined from the "isothermal" experiments characterised by the same dynamical parameters, thus yielding $h_2 = h_{iso}$. Combining Eqs. (2) and (3), it is easy to conclude that the remaining heat transfer coefficients may be calculated from $h_j = h_1$ and $h_c = h_2 + h_1 = h_{iso} + h_j$. The results obtained for the streamwise evolution of h_c and h_j are also shown in Fig. 6a–c. Both coefficients exhibit the classical evolution with the distance to the jet exit and very high values are obtained for h_c shortly after the jet exit. In addition, the heat transfer coefficient h_j, which accounts for the difference between h_c and h_{iso}, seems to attain negligible values for large x/d. This is in agreement with the view that the contribution of the cold jet vanishes as it mixes with the hot stream.

5. Conclusions

The main findings of the present experimental study on a non-isothermal, two-dimensional T-junction operating at a low value of momentum flux ratio may be summarised as follows:

1. The earlier development of large-scale structures in the interface between the jet and the cross-flow for the higher values of the Reynolds number translated into higher cooling effectiveness;
2. The formation of those organised structures is inhibited by the use of an upstream grid turbulator;
3. At the lowest value of the Reynolds number the dynamics of the flow was markedly different, thus suggesting a distinct regime of operation of the T-junction;
4. The arbitrary choice of the cross-flow temperature as a single reference produced an unusual behaviour of the heat transfer coefficient, generally increasing with the distance to the jet exit;
5. This difficulty has been circumvented by the definition of additional heat transfer coefficients, which allowed to take into consideration the temperature of the jet as well, and facilitated the physical interpretation of the results.

Acknowledgements

Part of this work is based on the experimental results obtained for a Ph.D. thesis (de Tilly [3]), which was supported by Areva–Framatome and CNRS-LET. Special thanks are given by the first author (A. de Tilly) for the help of his advisor, François Penot (CNRS-LET).

References

[1] S. Hahn, H. Choi, Unsteady simulation of jets in a cross flow, J. Comput. Phys. 134 (2) (1997) 342–356.

[2] T.F. Fric, A. Roshko, Vortical structure in the wake of a transverse jet, J. Fluid Mech. 279 (1994) 1–47.
[3] A. de Tilly, Contribution à l'étude des instabilités à la confluence d'écoulements non isothermes, PhD thesis, University of Poitiers, France, 2006.
[4] J.S. Anagnostopoulos, D.S. Mathioulakis, Unsteady flow field in a square tube T-junction, Phys. Fluids 16 (11) (2004) 3900–3910.
[5] V. Scherer, S. Wittig, The influence of the recirculation region: a comparison of the convective heat transfer downstream of a backward-facing step and behind a jet in a crossflow, J. Eng. Gas Turb. Power 113 (1991) 126–134.
[6] T. Fukuda, A. Sakashita, J. Mizutani, T. Matsunaga, K. Ogura, K. Shiina, K. Tanimoto, M. Shoichi, H. Madarame, Current effort to establish a JSME code for the evaluation of high-cycle thermal fatigue, in: Proceedings of the Eleventh International Conference on Nuclear Engineering, Tokyo, Japan, 2003.
[7] J.V. Beck, B. Blackwell, A. Haji-Sheikh, Comparison of some inverse heat conduction methods using experimental data, Int. J. Heat Mass Transf. 39 (17) (1996) 3649–3657.
[8] K. Ogura, Evaluation of unsteady heat transfer coefficient using a power spectrum method – prediction method of heat transfer coefficient, in: Proceedings of the Annual Meeting of the Atomic Energy Society of Japan, I40, Hokaido, Japan, 2001 (in Japanese).
[9] H. Noguchi, K. Tanimoto, Y. Kondo, H. Ishiga, K. Ogura, K. Shiina, Y. Minami, T. Fukuda, S. Moriya, H. Madarame, Study on high-cycle fatigue evaluation for thermal striping in mixing tees with hot and cold water, in: Proceedings of the Eleventh International Conference on Nuclear Engineering, Tokyo, Japan, 2003.
[10] E.R.G. Eckert, R.J. Goldstein, W.E. Ibele, S.V. Patankar, T.W. Simon, N.A. Decker, H. Lee, S.L. Girshick, P.J. Strykowski, K.K. Tamma, A. Bar-Cohen, J.V.R. Heberlein, Heat transfer – a review of 1989 literature, Int. J. Heat Mass Transf. 33 (11) (1990) 2349–2437.
[11] D. Maillet, Les limites du coefficient h: deux exemples aux temps courts et aux petites échelles, in: J. Padé, C. Bissieux, C. Padet, M. Lachi, H. Pron (Eds.), Actes du Congrès Annuel de la Société Française de Thermique, vol. 2, Reims, France, 2005, pp. 207–217.
[12] T.V. Jones, Definition of heat transfer coefficient in the turbine situation, IMechE Paper, C 423/046, Institution of Mechanical Engineers, 1991.
[13] C.H.N. Yuen, R.F. Martinez-Botas, Film cooling characteristics of a single round hole at various streamwise angles in a crossflow, Part I: effectiveness, Int. J. Heat Mass Transf. 46 (2003) 221–235.
[14] Z.D. Husain, A.K.M.F. Hussain, Natural instability of free shear layers, AIAA J. 21 (11) (1983) 1512–1517.
[15] L.W. Sigurdson, The structure and control of a turbulent reattaching flow, J. Fluid Mech. 298 (1995) 139–165.
[16] R.J. Goldstein, T. Yoshida, Boundary layer and laminar injection on film cooling performance, J. Heat Transf. 104 (1982) 355–362.